Antioxidant Activity and Stability of Purified Flavonoid Fractions from *Rosa davurica* Pall

Libu Niu [a], Jinping Zheng [a], Ruijian Wang [b] and Yanqiu Liu [a,b,*]

An ultrasound-assisted deep eutectic solvent was used to extract flavonoids from *Rosa davurica* Pall., followed by purification on macroporous resin; the separation and purification conditions were optimized. A total of 26 different flavonoid components were identified using ultraviolet spectroscopy, infrared spectroscopy, and ultra-high performance liquid chromatography-mass spectrometry. The antioxidant activity of purified flavonoids was significantly improved, as it not only exhibited excellent scavenging efficiency against DPPH radicals,·OH radicals, O^{2-} radicals, and $ABTS^{+}$ radicals, but also possessed strong total reducing power. Moreover, its antioxidant activity showed a clear positive correlation with concentration. This study provided a scientific basis for the comprehensive utilization of *Rosa davurica* Pall.

DOI: 10.15376/biores.21.3.7454-7474

Keywords: Total flavonoids; Rosa davurica Pall; Separation and purification; Ingredient; Antioxidant activity; Stability

Contact information: a: Forestry College of Beihua University of China, Jilin 132013, China; b: Engineering Research Center of Forestry Biotechnology of Jilin Province of China, Jilin 132013, China;
** Corresponding author: lyq800122@126.com*

INTRODUCTION

Rosa davurica Pall, belonging to the genus *Rosa* in the Rosaceae family and known as wild rose hip, is a wild deciduous shrub primarily distributed in South Korea, northeastern China, Siberia, Japan, and other regions of East Asia. The leaves, stems, fruits, and roots of *R. davurica* have been widely used in traditional herbal medicine for centuries. *Rosa davurica* contains various bioactive components, including flavonoids, polyphenols, triterpenes, tannins, polysaccharides, organic acids, vitamin C, amino acids, proanthocyanidins, and anthocyanins (Zhang *et al*. 2025). It has a long history of application in folk medicine. According to the records in the Compendium of Chinese Herbal Medicines and Heilongjiang Chinese Medicinal Materials, it can be used to treat indigestion, abdominal pain, diarrhea, stomachache, irregular menstruation, and other diseases (Zhao *et al*. 2024). Previous studies have demonstrated that *R. davurica* exhibits a variety of biological activities, including hypoglycemic, lipid-lowering, antioxidative, anti-allergic, and myocardial ischemia-improving effects (Hwang *et al*. 2024). (Kim *et al*. 1999; Shen *et al*. 2021; Liu *et al*. 2024; Yi *et al*. 2025)With the global demand for plant extract products on the rise, extracting high-purity, active, safe, and non-toxic natural flavonoids from plants have become a hot spot in the research and development of natural medicines (Cao *et al*. 2017). In recent years, quercetin and its glycoside derivatives (epigallocatechin and esters), as well as proanthocyanidin dimers, have become research hotspots due to their unique molecular structures (Nguyen and Bhattacharya 2022). These

compounds not only possess potent and diverse biological activities, which can precisely meet the intervention needs of high-incidence diseases such as tumors, neurodegenerative disorders, and metabolic syndrome, but they also have significant advantages such as wide natural sources, the ability to improve bioavailability through technological means, and broad industrial prospects (Thupakula *et al.* 2024). The flavonoids from the fruit of *Rosa davurica* are abundant, thus demonstrating great potential for applications in natural medicine and functional foods.

The current methods for extracting flavonoids mostly involve water extraction and ethanol reflux. These methods have problems such as low extraction efficiency, residual solvents, and the easy degradation of active components. In this study, ultrasonic-assisted deep eutectic solvent extraction was introduced. By leveraging its non-toxicity, low volatility, and high thermal stability, this method has improved extraction efficiency while preserving the components' activity (Gao *et al.* 2025a). Utilizing the ultrasonic cavitation effect to break cells accelerates the release of flavonoids and achieves the green and efficient extraction of flavonoids from *R. davurica*. The current purification methods mostly rely on simple, crude separation, without systematic optimization of parameters for macroporous resin purification. As a result, the purity of the obtained flavonoids is low. In this study, a macroporous resin was used for purification, and the process parameters were optimized using single-factor experiments, significantly improving flavonoid purity. Oxidative stress is caused by the generation of reactive oxygen and reactive nitrogen species that exceeds the clearance capacity, and it can induce various diseases. Flavonoids exert antioxidant effects by removing free radicals through phenolic hydroxyl groups, and they play an important role in preventing various chronic diseases (Gao *et al.* 2025b).

At present, research on the antioxidant properties of flavonoids from *Rosa davurica* is rather limited. Most studies have focused on only one or two types of free radicals, making it difficult to objectively demonstrate their advantages. This article systematically assessed the scavenging ability of *R. davurica* against DPPH, ·OH, O^{2-}, and $ABTS^{+}$ free radicals and compared it with that of vitamin C as a control, providing a scientific basis for its use as a natural antioxidant.

This study, for the first time, adopted a deep eutectic solvent combined with ultrasonic-assisted extraction to extract flavonoids from *Rosa davurica*. Meanwhile, it optimized the macroporous resin purification process using single-factor experiments. Furthermore, using ultraviolet-visible spectroscopy, Fourier transform infrared spectroscopy, and ultra-high-performance liquid chromatography-mass spectrometry (UHPLC-MS), this study identified 26 flavonoid compounds from *R. davurica* and verified their antioxidant capacity through *in vitro* antioxidant assays.

EXPERIMENTAL

Materials and Reagents

Rosa davurica Pall., a wild plant, was harvested from Changbai Mountain in Jilin Province. According to the "Flora of China" compiled by Professor Chen Xiaqiang of Northeast Forestry University, it was identified as *Rosa davurica* Pall.

Choline chloride, ethylene glycol, glucose, sucrose, anhydrous ethanol, rutin, potassium persulfate, ferrous sulfate, catechin, xylenol orange, salicylic acid, methanol, and acetonitrile were sourced from Beijing Solarbio Science and Technology Co., Ltd.

(Beijing, China). Macroporous resins D101, NKA-9, AB-8, HP20, and HPD-1008 (varying polarities) were obtained from Beijing Sollebo Technology Co., Ltd. (Beijing, China). DPPH (1,1-diphenyl-2-nitrobenzhydrazide) was purchased from Foshan Maiqing Chemical Co., Ltd. (Foshan, China) ABTS (2,2'-azinobis(3-ethylbenzothiazoline-6-sulfonic acid)) was acquired from Aladdin Biotechnology Co., Ltd. (Shanghai, China); L-ascorbic acid (Vc) was obtained from Hunan Aite Scientific Instrument Co., Ltd. (Hunan, China); hydrogen peroxide, Tris-HCl buffer were purchased from Shenzhen Fulin Instrument Technology Co., Ltd. (Shenzhen, China).

Preparation of Low-Solvent-Mixing Extraction Solution

A deep eutectic solvent (DES) composed of choline chloride and ethylene glycol (molar ratio 1:4) with a water content of 20% was used to extract flavonoids from *Rosa davurica* Pall (RDP). About 2 g of *R. davurica* powder was weighed and added to the DES solution at a liquid-to-solid ratio of 1:10. The blend was fully mixed and then transferred to a water bath maintained at 40 ℃ for extraction for 1 h. Next, ultrasonic processing was conducted at 20 kHz and 300 W for 30 min in pulse intermittent mode. The mixture was centrifuged at 8000 ×g for 10 min to collect the DES extract. Subsequently, the extract was evaporated and concentrated using a rotary evaporator at 50 ℃, and the concentrated solution was stored for future use.

Separation and Purification of Flavonoid Compounds

Pretreatment of macroporous resins

Five macroporous resins, D101, NKA-9, AB-8, HP20, and HPD-100, were soaked in 95% ethanol for 24 h to achieve complete expansion. Afterward, the resins were thoroughly rinsed with distilled water to remove any alcohol smell. Subsequently, the resins, immersed in 5% HCl for 3 h, were washed with distilled water until neutral. Subsequently, they were exposed to a 5% NaOH solution for 3 h, rinsed to neutrality, and prepared for use.

Screening of macroporous resins

Two grams of each of the five pretreated macroporous resins (D101, NKA-9, AB-8, HP20, HPD-100) were accurately weighed and placed in 50 mL Erlenmeyer flasks. Subsequently, 30 mL of the flavonoid extract at 0.5 mg/mL was added to each flask. The mixtures were thoroughly homogenized and then transferred to a shaking incubator for static adsorption at 25 ℃ and 100 rpm for 6 hours. After adsorption, the resin was separated from the solution by suction filtration, and the RDP content in the post-adsorption extract was determined. The resin surface was rinsed with distilled water to remove the floating color. Thereafter, 30 mL of 70% ethanol solution was used for desorption, and the desorption process was carried out for 6 hours. Upon the end of desorption, the ethanol desorption solution was separated from the resin by suction filtration, and the flavonoid content in the desorption solution was measured. The adsorption and desorption percentages of different types of macroporous resins were calculated using the following formulas.

$$\%\ \text{Adsorption rate} = \frac{C_0 - C_1}{C_0} \times 100\% \quad (1)$$

$$\%\ \text{Desorption rate} = \frac{C_2 V_2}{(C_0\text{-}C_1)\ V_1} \times 100\% \quad (2)$$

In Eqs. 1-2, C_0 is the initial concentration of flavonoids in the sample solution (mg/mL), C_1 is the concentration of flavonoids in the effluent, C_2 is the concentration of flavonoids in the eluent, V_1 is the volume of the sample solution, and V_2 is the volume of the eluent.

Static adsorption kinetic experiment

About 2 g of the preferred macroporous resin was added to 50 mL of the flavonoids from the *Rosa davurica* Pall crude extract at a concentration of 0.5 mg/mL. The mixture was transferred to a 100 mL conical flask and shaken at 25 ℃ with a rotation speed of 120 rpm. Regular samples were withdrawn to monitor concentration, and a static adsorption kinetic curve was constructed by plotting the adsorption percent against time.

Static desorption kinetic experiment

The macroporous resin, post-adsorption, was filtered and then added to 50 mL of ethanol in a 100 mL conical flask. This flask was then positioned in a shaker at 25 ℃, operating at 100 rpm for desorption. Periodic sampling was conducted to quantify the substance's concentration. The desorption percent was graphed on the Y-axis against desorption time on the X-axis to construct the static desorption curve.

Single-factor experiments of the purification process

The effects was investigated of different injection flow rates (1.0, 2.0, 3.0, 4.0, 5.0 mL/min), injection concentrations (0.25, 0.50, 0.75, 1.00, 1.25 mg/mL), and pH values (2, 3, 4, 5, 6) on the adsorption percent of RDP, as well as the effects of different elution concentrations (50%, 60%, 70%, 80%, 90%) and elution flow rates (1.0, 2.0, 3.0, 4.0, 5.0 mL/min) on the desorption percent of RDP. Leak curves and elution volumes were also plotted.

Physical and Chemical Properties Analysis of *Rosa davurica* Pall (RDP)

Ultraviolet spectral analysis

The ultraviolet characteristic absorbance peaks of flavonoid compounds were determined by ultraviolet spectral scanning. A flavonoid standard solution was prepared with 70% ethanol. The properly diluted sample extract was transferred into a test tube for color reaction. Briefly, 5% sodium nitrite solution was added, mixed thoroughly, and incubated for 6 min, followed by the addition of 10% aluminum nitrate solution with another 6 min of standing. Afterward, 1 mol/L sodium hydroxide solution was supplemented, and the crude extract was transferred into a volumetric flask, diluted to constant volume with 70% ethanol and stored away from light for 30 min to reach the required concentration. With the reagent blank as the reference, the UV–Vis absorption spectrum was scanned over the wavelength range of 400–600 nm, and the absorbance value at approximately 510 nm.

Infrared spectral analysis

The characteristic functional groups of flavonoid compounds were analyzed by infrared spectral scanning. About 100 mg of potassium bromide was ground and mixed

evenly with 1 mg of purified flavonoid powder. The mixture was pressed into a sample and placed in an infrared spectrometer to detect in the 4000 to 5000 cm^{-1} range.

HPLC-MS identification and analysis

The flavonoids in RDP were preliminarily identified and qualitatively analyzed using HPLC-MS. A known mass of the RDP sample was accurately weighed and placed in a volumetric flask, and then methanol was added to dissolve it. An aliquot of 1 mL of the resultant solution was filtered through a microporous membrane, transferred to another volumetric flask, and diluted to a final volume of 1.5 mL. Chromatographic conditions for liquid chromatography: The separation was performed on an Acquity UPLC BEH C_{18} column (2.1 × 50 mm, 1.7 μm, Waters, USA). The injection volume was set at 10 μL, and the column temperature was maintained at 40 ℃. Mobile phase A was a 0.1% formic acid aqueous solution, and mobile phase B was a 0.1% formic acid acetonitrile solution. Gradient election was implemented according to the procedure detailed in Fig. 4 and Table 1. Mass spectrometric conditions: The mass spectrometer was operated in both positive and negative electrospray ionization (ESI) modes. The ionization voltage was 3500 V in positive mode and -2500 V in negative mode. The desolvation gas temperature was set at 350 ℃, and the ion transfer tube temperature was 320 ℃. The sheath gas flow rate was 40 arb, and the auxiliary gas flow rate was 15 arb. Compounds were identified by comparing the retention times and UV spectra of peaks with those of authentic standards.

Research on the Antioxidant Activity of *Rosa davurica* Pall (RDP)

Determination of DPPH radical scavenging capacity

The DPPH radical scavenging activity was measured by preparing sample solutions at concentrations ranging from 0.01 to 0.05 mg/mL. For each assay, 4.0 mL of sample solution was mixed with 2.0 mL of freshly prepared 0.2 mmol/L DPPH solution in a stoppered test tube. After thorough vortexing, the mixture was incubated in the dark for 30 minutes. Using ascorbic acid (Vc) as a positive control, absorbance was measured at 517 nm, and the scavenging percent was calculated according to a published method (Diao *et al.* 2025).

$$\% \text{ Scavenging activity} = (1-\frac{A_1-A_2}{A_3})\times 100\% \quad (3)$$

In Eq. 3, A_1 is the absorbance value of the flavonoid solution, A_2 is the absorbance value when methanol is used instead of DPPH, and A_3 is the absorbance value when the flavonoid solution is replaced by distilled water.

Determination of ·OH radical scavenging capacity

Sample solutions at concentrations of 0.1 to 0.5 mg/mL were prepared for analysis. In each reaction, 1 mL of a 9 mmol/L $FeSO_4$ solution, 1 mL of a 9 mmol/L salicylic acid ethanol solution, 1 mL of the sample solution, and 1 mL of an 8.8 mmol/L H_2O_2 solution were sequentially added to a test tube and mixed thoroughly. The mixture was then incubated at 37 ℃ for 30 min to initiate the reaction. Using ascorbic acid (Vc) as the positive control, absorbance was measured at 510 nm, and the scavenging percent was calculated using the method of Li *et al.* (2024).

$$\% \text{ Scavenging activity} = (1-\frac{A_4-A_5}{A_6})\times 100\% \quad (4)$$

In the formula: A_4 is the absorbance value of the flavonoid solution, A_5 is the absorbance value when distilled water is used instead of H_2O_2, and A_6 is the absorbance value when distilled water is used instead of the flavonoid solution.

Determination of O^{2-} radical scavenging capacity

Sample solutions ranging from 0.1 to 0.5 mg/mL were prepared and stored. In a 10 mL stoppered test tube, 3.0 mL of Tris-HCl buffer (50 mmol/L, pH 8.2) was first incubated at 25 ℃ for 20 min. Subsequently, 2.0 mL of the sample solution and 2.0 mL of a 30 mmol/L pyrogallol solution were thoroughly added, and the mixture was incubated for another 8 min at 25 ℃. The reaction was terminated by adding one drop of 10 mmol/L HCl. Using Tris-HCl buffer as the blank and ascorbic acid (Vc) as the positive control, absorbance was measured at 320 nm, and the scavenging percent was calculated using the corresponding formula (Zhang *et al.* 2016).

$$\% \text{ Scavenging activity} = 1-\frac{A_7-A_8}{A_9}\times 100\% \quad (5)$$

In the formula: A_7 is the absorbance value of the flavonoid solution, A_8 is the absorbance value when distilled water is used instead of the resorcinol solution, and A_9 is the absorbance value when distilled water is used instead of the flavonoid solution.

Determination of $ABTS^+$ scavenging ability

Sample solutions ranging from 0.004 to 0.020 mg/mL were prepared and stored. The $ABTS^+$ working solution was prepared by mixing equal volumes of 7 mmol/L ABTS solution and 2.45 mmol/L potassium persulfate solution, then incubated in the dark for 12 h. The solution was then diluted 50-fold with absolute ethanol to reach an absorbance of 0.7 ± 0.02 at 734 nm. For the assay, 0.1 mL of sample solution was added to 3.9 mL of the $ABTS^+$ working solution, and the mixture was incubated at room temperature for 6 min. Using absolute ethanol as the blank and ascorbic acid (Vc) as the positive control, absorbance was measured at 734 nm, and the scavenging percent was calculated using Eq. 6 (Liu *et al*. 2024).

$$\% \text{ Scavenging activity} = \frac{A_{10}-A_{11}}{A_{10}}\times 100\% \quad (6)$$

In the formula, A_{10} is the absorbance value when absolute ethanol replaces the flavonoid solution, and A_{11} is the absorbance value of the flavonoid solution.

Statistical Analysis

All experiments were performed in triplicate, and outcomes were expressed as the mean ± SD. Data were analyzed employing one-way ANOVA followed by Origin 2024. Different superscript letters show significant differences at $P \leq 0.05$.

RESULTS AND DISCUSSION

Separation and Purification of *Rosa davurica* Pall (RDP)

Screening of macroporous resins

Five different polar macroporous resins were chosen for static adsorption and desorption tests in this study, as shown in Fig. 1. Distinct molecular adsorption resins (MARs) exhibit varying capacities for flavonoid compounds due to their diverse physical properties. The MARs separate compounds based on hydrogen bonding and van der Waals forces with the adsorbed substance. The selective adsorption of MARs underscores the importance of prioritizing those with superior flavonoid adsorption. Furthermore, the desorption efficiency of MARs indicates their regeneration potential and determines the recoverable flavonoid quantity post-adsorption (Chen *et al.* 2025). The AB-8 resin exhibited an adsorption efficiency of 90.6% for RDP, outperforming the other resins. This may be attributed to the fact that both the AB-8 resin and the total flavonoids in RDP are weakly polar substances, and the average pore size of the AB-8 resin is larger than that of the other tested resins, thereby enabling better adsorption and desorption of the total flavonoids in RDP. AB-8 resin exhibited a desorption percent of 94.4%, significantly surpassing those of other resins, making it a preferred choice for RDP separation.

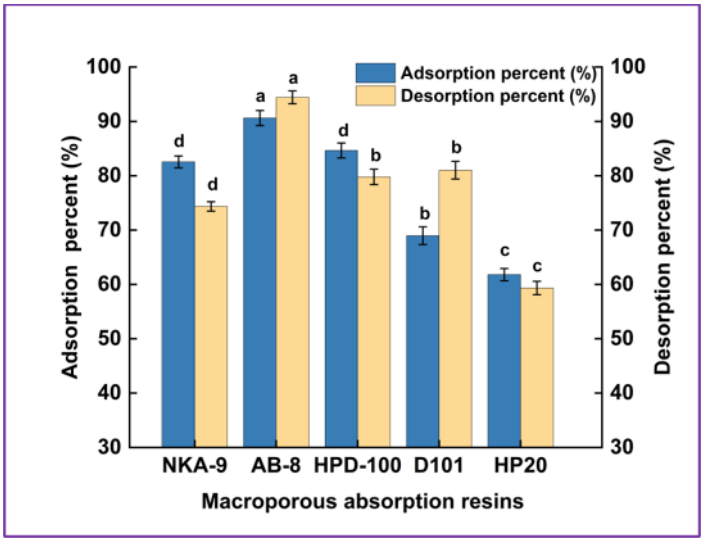

Fig. 1. Adsorption/desorption capacities and desorption percentages for flavonoids on different resins. Different superscript letters within the same row denote significant differences ($P \leq 0.05$).

Kinetics curves for static adsorption and desorption of AB-8.

The kinetics curves of total flavonoids in RDP extract were investigated using AB-8 macroporous resin, which is known for its rapid adsorption and desorption percent. Figure 2(A) illustrates the swift adsorption of a substantial amount of flavonoids by MARs within 2 h, with the adsorption percent approaching saturation and achieving equilibrium after 1.0 h. Conversely, Fig. 2(B) shows the rapid release of flavonoids within 2 h, with equilibrium reached after one hour. Consequently, the optimal adsorption and desorption times for AB-8 macroporous resin were determined to be 2 h and 3 h, respectively.

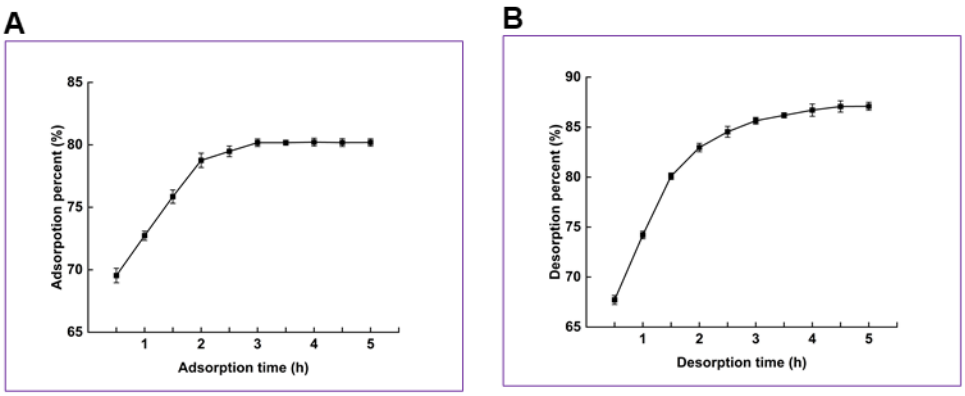

Fig. 2 (A-B). Kinetics curves for static adsorption and desorption percent of AB-8. (A) Effect of adsorption time on adsorption percent; (B) Effect of desorption time on desorption percent

Single-factor experiments of the purification process

Figure 3(A) illustrates that as the sample injection flow rate rises, the adsorption percent decreases gradually. A higher injection flow percentage leads to shorter contact times between tree fruit flavonoids and the macroporous resin, resulting in some target substances failing to interact fully with the resin and eluting from the column, thereby reducing adsorption. Between 1.0 and 2 mL/min, changes in the sample injection flow percent have minimal impact on the adsorption percent. At 1.0 mL/min, operational efficiency decreases; hence, a flow rate of 2 mL/min is chosen. Hence, a flow rate of 2 mL/min is chosen as the ideal condition for purifying the samples in future studies.

As illustrated in Fig. 3(B), the adsorption amount initially increased and then declined with increasing sample concentration. At a concentration of 5 mg/mL, the adsorption percentage reached 87.3%. As the concentration increased, the adsorption percent continued to decrease. This may be because when the sample concentration is high, the solution's viscosity increases, leading to greater diffusion resistance for flavonoid molecules. This impedes their engagement with active sites on the resin surface, leading to incomplete adsorption. Moreover, excessive concentration results in elevated impurity levels that occupy the resin's accessible active sites, weaken the adsorption force between the flavonoid compounds and the resin, and reduce the resin's adsorption capacity. A lower sample concentration will increase the purification time and reduce the purification efficiency. Thus, selecting a sample concentration of 5 mg/mL is deemed optimal for the purification process in further studies.

In Fig. 3(C), the adsorption percent increased gradually as the pH rose from 3 to 5. At pH 5, the adsorption percent reached 86.7% for the AB-8 macroporous resin. With further increases in pH, the adsorption percent declined gradually. This trend could be attributed to the acidic nature of flavonoid compounds, which commonly feature phenolic hydroxyl and carboxyl groups that ionize to varying degrees with pH. Optimizing pH can enhance interactions between flavonoids and functional groups on MARs. At pH 5, the phenolic hydroxyl groups of flavonoid molecules were only partially dissociated, and the overall polarity of the molecules was moderate. The hydrophobic and hydrogen-bond interactions with the macroporous resin were the strongest. At extreme pH values, the surface functional groups of the macroporous resin may be protonated, reducing its affinity for flavonoid compounds and slowing adsorption. Thus, pH 5 was selected as the ideal purification condition for further study.

In Fig. 3(D), at an injection volume of 90 mL, the effluent's total flavonoid concentration was 0.042 mg/mL, which was less than 10% of the initial injection solution concentration. This suggests thorough adsorption of total flavonoids by the resin at this stage. However, when the injection volume exceeded 90 mL, as the active sites of the resin gradually became saturated, its adsorption capacity for the target substance decreased, and the effluent's flavonoid concentration rose swiftly as the target substance concentration in the effluent hit 10% of the injection solution's initial concentration, marking the leakage point. This indicates that 90 mL represents the critical point of leakage for the adsorption process. Hence, the ideal sample solution injection volume was 90 mL.

Figure 3(E) illustrates a gradual increase in the desorption percent with increasing ethanol volume fraction from 50% to 70%. At 70% ethanol volume fraction, the desorption percent peaked at 91.2%. Subsequently, as the ethanol volume fraction increased, the desorption percent gradually declined. This is because ethanol breaks hydrogen bonds between flavonoids and the resin, thereby enhancing their solubility and promoting their desorption. In low-concentration solutions, ethanol molecules have their hydroxyl groups occupied by water molecules, hindering their effective competition with the active sites on the resin surface. This limitation prevents them from fully disrupting the hydrogen bond between flavonoids and the resin, thereby reducing desorption efficiency. When the ethanol volume fraction reached 70%, the overall polarity of the ethanol-water mixture was close to that of RDP. According to the "like dissolves like" principle, RDP achieved maximum solubility and optimal desorption efficiency at this ethanol concentration. As the ethanol content continued to increase, the overall polarity of the mixed solvent declined. Low-polarity, high-concentration ethanol reduced flavonoid solubility. Meanwhile, excessive ethanol shrank the resin pore structure and strengthened the hydrophobic interaction between the resin and flavonoids, resulting in a reduced desorption percentage. Hence, the optimal purification condition for further research was selected as 70% ethanol.

Figure 3(F) illustrates a pattern where the desorption percent initially rose, then declined as the elution flow percent increased. At a flow rate of 2 mL/min, the desorption percent peaked at 91.5%. The elution flow rate significantly influenced the desorption percent; an inadequate flow rate resulted in sluggish eluent flow, and the mass transfer driving force for flavonoid molecules to diffuse from the resin pores into the solution was insufficient. Certain flavonoids may re-adsorb onto the resin due to prolonged residence time; conversely, a high elution flow rate can result in insufficient contact with the resin, thereby decreasing the desorption percent. Hence, an elution flow rate of 2 mL/min is deemed optimal for subsequent purification studies.

Figure 3(G) illustrates that flavonoid concentration peaks at an elution volume of 20 mL. As the elution solution volume increases, RDP content in the effluent also rises gradually. At 20 mL of ethanol solution volume, the content of flavonoids in the elution solution reaches its maximum, and then gradually decreases. Flavonoids adsorbed on the AB-8 macroporous resin are eluted when the elution volume surpasses 100 mL, nearing the elution endpoint. Hence, the ideal elution volume is set at 100 mL.

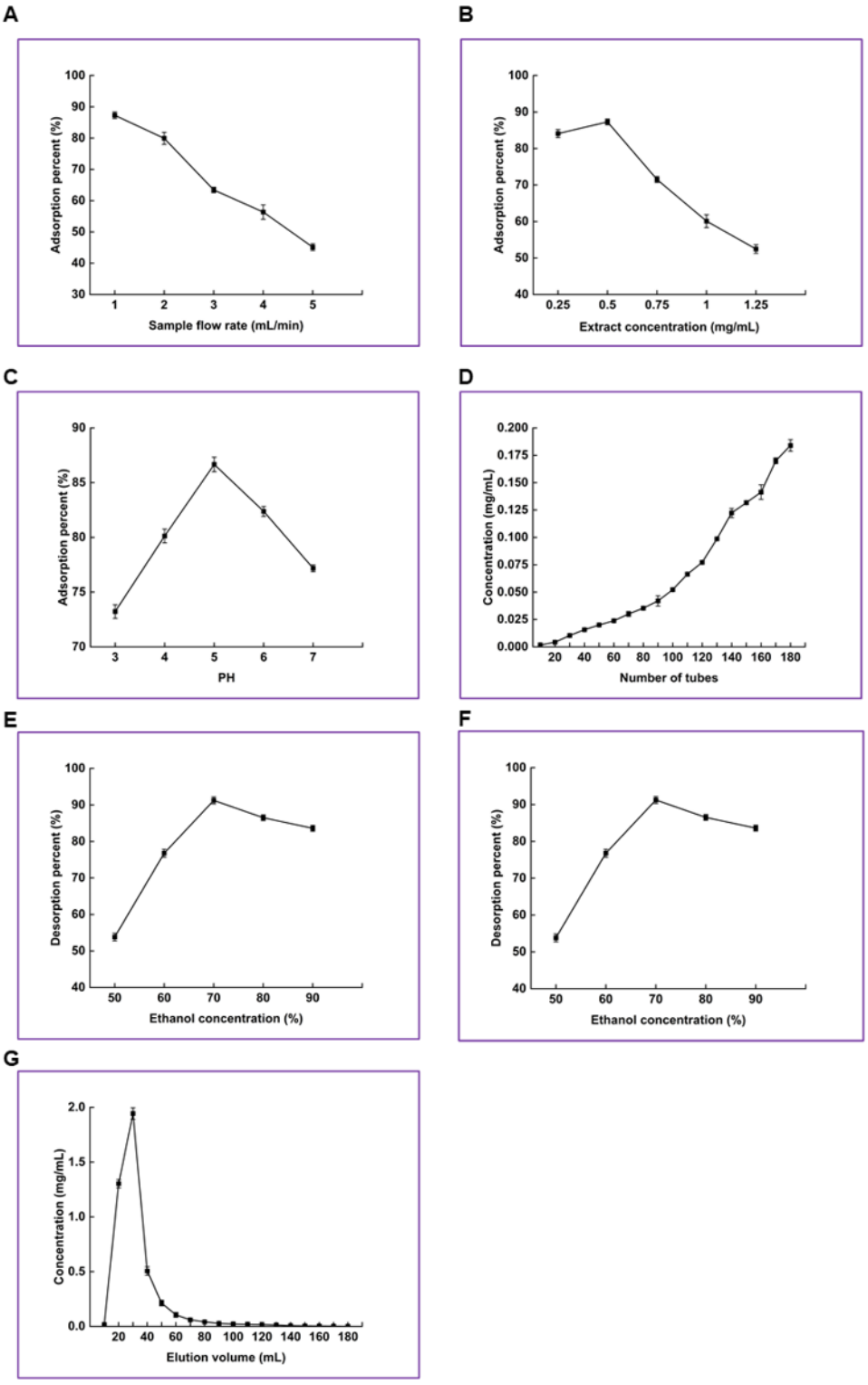

Fig. 3 (A-G). The results of the single-factor tests for the purification process: (A) Effect of sample injection flow rate on adsorption percent; (B) Effect of sample concentration on adsorption percent; (C) Effect of sample pH on adsorption percent; (D) Leakage curve; (E) Effect of elution concentration on desorption percent; (F) Effect of elution flow rate on desorption percent; and (G) Effect of elution volume on desorption rate.

Qualitative Analysis of Flavonoid Components

Ultraviolet-visible spectral analysis

The UV-Vis spectral analysis was conducted within the wavelength range of 200 to 800 nm to scan the characteristic absorbance peaks of the radiation. The results are shown in Fig. 4(A). At around 500 nm, a strong absorbance peak is observed in the UV-spectrum. The 26 identified components mainly include flavonoids, flavonols, flavanones, procyanidins, phenolic acids, and tannins. Some of these compounds have conjugated structures and polyphenol polymerization characteristics. This analysis indicates that the ultraviolet-visible spectrum of the purified RDP substance is characteristic of flavonoid spectra. It is speculated that this compound contains flavonoid compounds.

Infrared spectroscopy analysis

Using a Fourier transform infrared spectrometer, one can analyze the extract and determine whether it contains flavonoids based on characteristic functional groups, such as phenolic hydroxyl groups, carbonyl groups, benzene rings, and ether bonds. Figure 4(B) illustrates the infrared spectrum of the sample, indicating that the 3700 to 2500 cm^{-1} range predominantly showed absorbance peaks corresponding to X-H bond-stretching vibrations. Two absorbance peaks are evident, potentially arising from overlapping multiple-OH stretching vibrations at 3394.7 cm^{-1}. The intense and broad absorbance peak at 2925.01 cm^{-1} corresponds to the C-H stretching vibration, while 1522.1 cm^{-1} represents the carbonyl group's stretching vibration absorbance peak, and 1602.0 cm^{-1}. The absorbance peaks at 1448.7 cm^{-1} correspond to the C=C stretching vibration in the aromatic ring, while those at 1285.0 cm^{-1} represent the C-O-C stretching vibration in the ether. Additionally, the peak at 1073.8 cm^{-1} indicates the stretching vibration of the phenolic hydroxyl group, and the peak at 820.6 cm^{-1} corresponds to the β-glycosidic bond. This suggests the presence of flavanol-type compounds with a benzene ring structure containing phenolic hydroxyl groups.

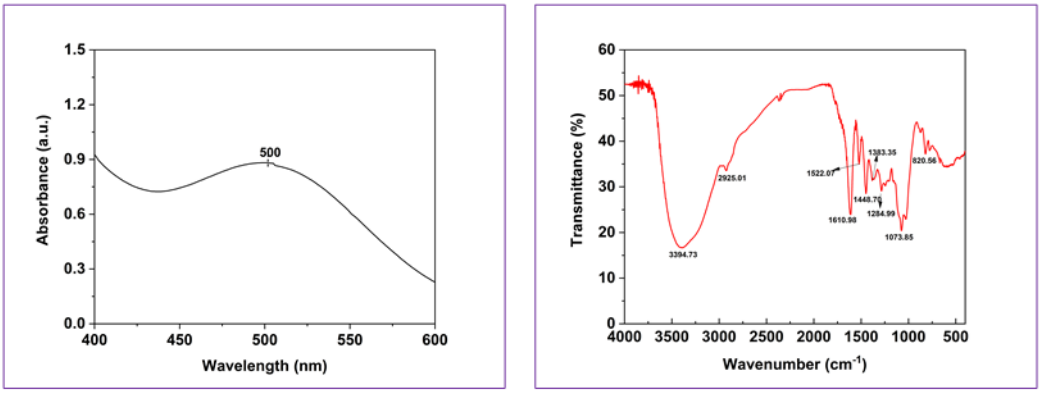

Fig. 4 (A-B). The ultraviolet spectrum and infrared spectrum of RDP: (A) Ultraviolet spectrum of RDP; (B) Infrared spectrum of RDP

HPLC-MS Identification and Analysis

The flavonoids in RDP were qualitatively analyzed and preliminarily identified using HPLC-MS in ESI-positive and negative ion modes. Identification using the mzVault database (OTCML) revealed 26 flavonoids. Total ion current chromatograms for positive and negative ion modes are depicted in Figs. 5(A) and 5(B). Identification outcomes and chemical structures are displayed in Tables 3 and 4, respectively. Among the top ten

flavonoids with higher contents are epicatechin, quercetin, isoquercitrin, quercetin-3-glucuronide, epigallocatechin, proanthocyanidin B_2, dihydroquercitrin, rhamnetin, rutin, and naringenin.

As shown in Fig. 5, the molecular ion peak $[M-H]^{-1}$ of RDP-1 is 289.07162, which, based on comparison with the mzVault database, is inferred to be epicatechin and corresponds to the molecular formula $C_{15}H_{14}O_6$. RDP-2's molecular ion peak $[M-H]^{-1}$ is 301.03519, which, upon comparison with the mzVault database, is inferred as Quercetin, corresponding to the molecular formula $C_{15}H_{10}O_7$. RDP-3's molecular ion peak $[M-H]^{-1}$ is 463.08823, which, upon comparison with the mzVault database, is inferred as Isoquercitrin, with the molecular formula $C_{21}H_{20}O_{12}$. RDP-4's molecular ion peak $[M-H]^{-1}$ is 477.06729, inferred as Quercetin-3-O-β-D-Glucuronide by comparison with the mzVault database, with the molecular formula $C_{21}H_{18}O_{13}$. RDP-5's molecular ion peak $[M-H]^{-1}$ is 305.06671, inferred as (-)-Epigallocatechin (-)- by comparison with the mzVault database, with the molecular formula $C_{15}H_{14}O_7$. RDP-6's molecular ion peak $[M-H]^{-1}$ is 577.1358, inferred as Procyanidin B_2 by comparison with the mzVault database, with the molecular formula $C_{30}H_{26}O_{12}$. RDP-7's molecular ion peak $[M-H]^{-1}$ is 303.0509, which, by comparison with the mzVault database, is inferred as Dihydroquercetin, with the molecular formula $C_{15}H_{12}O_7$. RDP-8's molecular ion peak $[M-H]^{-1}$ is 435.12958, which, upon comparison with the mzVault database, is inferred as Phlorizin, with the molecular formula $C_{21}H_{24}O_{10}$. RDP-9's molecular ion peak $[M-H]^{-1}$ is 609.14667, which, based on comparison with the mzVault database, is inferred as Rutin and corresponds to the molecular formula $C_{27}H_{30}O_{16}$. RDP-10's molecular ion peak$[M-H]^{-1}$ is 271.061, inferred as Naringenin by comparison with the mzVault database, with the molecular formula $C_{15}H_{12}O_5$. RDP-11's molecular ion peak $[M-H]^{-1}$ is 287.05597, which, based on comparison with the mzVault database, is inferred as Eriodictyol and corresponds to the molecular formula $C_{15}H_{12}O_6$. RDP-12's molecular ion peak $[M-H]^{-1}$ is 353.08752, inferred as Chlorogenic acid by comparison with the mzVault database, with the molecular formula $C_{16}H_{18}O_9$. RDP-13's molecular ion peak $[M-H]^{-1}$ is 269.04544, which, based on comparison with the mzVault database, is inferred as Emodin and corresponds to the molecular formula $C_{15}H_{10}O_5$. RDP-14's molecular ion peak $[M-H]^{-1}$ is 549.16193, inferred as Liquiritigenin-7-O-β-D-apiofuranosyl-4'-O-β-D-glucopyranoside by comparison with the mzVault database, with the molecular formula $C_{26}H_{30}O_{13}$. RDP-15's molecular ion peak $[M-H]^{-1}$ is 299.01962, which, based on comparison with the mzVault database, is inferred as Demethylwedelolactone and has the molecular formula C15H8O7. RDP-16's molecular ion peak $[M-H]^{-1}$ is 441.08276, inferred as (-)-Epicatechin gallate (-)- by comparison with the mzVault database, with the molecular formula $C_{22}H_{18}O_{10}$. RDP-17's molecular ion peak $[M-H]^{-1}$ is 273.07666, which, by comparison with the mzVault database, is inferred as Phloretin, with the molecular formula $C_{15}H_{14}O_5$. RDP-18's molecular ion peak $[M-H]^{-1}$ is 461.07257, which is inferred as Scutellarin by comparison with the mzVault database, corresponding to the molecular formula $C_{21}H_{18}O_{12}$.

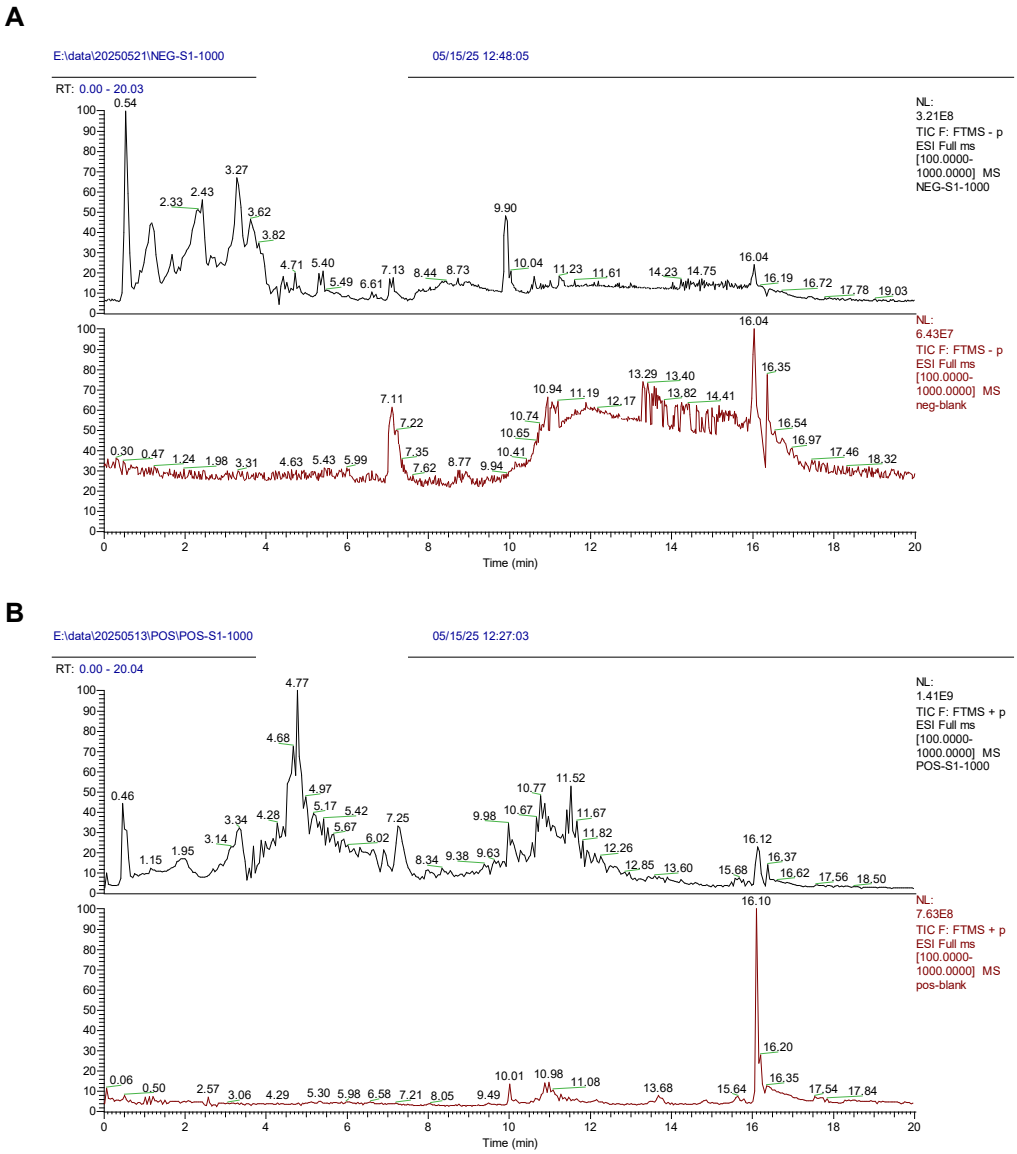

Fig. 5 (A-B). Total ion chromatograms of samples in negative ion and positive ion modes: (A) Total ion chromatogram of the sample (upper panel) and blank control (lower panel) in negative ion mode; and (B) Total ion chromatogram of the sample (upper panel) and blank control (lower panel) in positive ion mode

RDP-19's molecular ion peak $[M-H]^{+1}$ is 451.12372, which, based on comparison with the mzVault database, is inferred as Astilbin and has the molecular formula $C_{21}H_{22}O_{11}$. RDP-20's molecular ion peak $[M-H]^{+1}$ is 303.04977, inferred as Morin by comparison with the mzVault database, with the molecular formula $C_{15}H_{10}O_7$. RDP-21's molecular ion peak $[M-H]^{+1}$ is 579.15045, inferred as Procyanidin B_1 by comparison with the mzVault database, with the molecular formula $C_{30}H_{26}O_{12}$. RDP-22's molecular ion peak $[M-H]^{+1}$ is 617.11426, inferred as 2'-O-Galloylhyperin 2'-O- by comparison with the mzVault database, with the molecular formula $C_{28}H_{24}O_{16}$.

Table 1. HPLC/MS Data and Preliminary Identification Results of Flavonoid Components in *Rosa davurica* Pall

No.	Compound	Ion Mode	Formula	Retention Time (min)	Measured Value (m/z)	Theoretical Value (m/z)	Error (ppm)
1	Epicatechin	$[M-H]^{-1}$	$C_{15}H_{14}O_6$	2.713	289.07162	289.0711	-0.42
2	Quercetin	$[M-H]^{-1}$	$C_{15}H_{10}O_7$	4.727	301.03519	301.03465	-0.62
3	Isoquercitrin	$[M-H]^{-1}$	$C_{21}H_{20}O_{12}$	3.768	463.08823	463.08768	0.06
4	Quercetin 3-O-β-D-Glucuronide	$[M-H]^{-1}$	$C_{21}H_{18}O_{13}$	3.774	477.06729	477.06675	-0.36
5	Epigallocatechin (-)-	$[M-H]^{-1}$	$C_{15}H_{14}O_7$	1.179	305.06671	305.06617	0.11
6	Procyanidin B_2	$[M-H]^{-1}$	$C_{30}H_{26}O_{12}$	2.465	577.1358	577.13526	1.13
7	Dihydroquercetin	$[M-H]^{-1}$	$C_{15}H_{12}O_7$	3.821	303.0509	303.05036	-0.39
8	Phlorizin	$[M-H]^{-1}$	$C_{21}H_{24}O_{10}$	4.262	435.12958	435.12905	-0.19
9	Rutin	$[M-H]^{-1}$	$C_{27}H_{30}O_{16}$	3.671	609.14667	609.14612	0.92
10	Naringenin	$[M-H]^{-1}$	$C_{15}H_{12}O_5$	5.163	271.061	271.06046	-0.71
11	Eriodictyol	$[M-H]^{-1}$	$C_{15}H_{12}O_6$	4.701	287.05597	287.05543	-0.49
12	Chlorogenic acid	$[M-H]^{-1}$	$C_{16}H_{18}O_9$	3.216	353.08752	353.08698	-0.79
13	Emodin	$[M-H]^{-1}$	$C_{15}H_{10}O_5$	2.875	269.04544	269.0449	-0.39
14	Glycyrrhizinate-7-O-β-D-saccharose-4'-O-β-D-glucoside	$[M-H]^{-1}$	$C_{26}H_{30}O_{13}$	4.819	549.16193	549.16138	1.02
15	Demethylwedelolactone	$[M-H]^{-1}$	$C_{15}H_8O_7$	4.734	299.01962	299.01908	-0.34
16	(-)-Epicatechin gallate (-)-	$[M-H]^{-1}$	$C_{22}H_{18}O_{10}$	3.809	441.08276	441.08222	0.1
17	Phloretin	$[M-H]^{-1}$	$C_{15}H_{14}O$	5.18	273.07666	273.07612	-0.68
18	Scutellarin	$[M-H]^{-1}$	$C_{21}H_{18}O_{12}$	3.998	461.07257	461.0720	0.05
19	Astilbin	$[M+H]^{+1}$	$C_{21}H_{22}O_{11}$	1.905	451.12372	451.12426	0.51
20	Morin	$[M+H]^{+1}$	$C_{15}H_{10}O_7$	4.771	303.04977	303.05032	-0.51
21	Procyanidin B_1	$[M+H]^{+1}$	$C_{30}H_{26}O_{12}$	2.385	579.15045	579.151	1.3
22	2'-O-galactosylflavonoid	$[M+H]^{+1}$	$C_{28}H_{24}O_{16}$	3.673	617.11426	617.1148	0.8
23	Pinocembrin	$[M+H]^{+1}$	$C_{15}H_{12}O_4$	4.788	257.08072	257.08126	-0.45
24	(+)-Gallocatechin	$[M+H]^{+1}$	$C_{15}H_{14}O_7$	4.788	307.08133	307.08187	0.33
25	Myricetin	$[M+H]^{+1}$	$C_{15}H_{10}O_8$	4.205	319.04514	319.04568	0.92
26	Kaempferol-7-O-β-D-glucopyranoside	$[M+H]^{+1}$	$C_{21}H_{20}O_{11}$	2.915	449.10797	449.10851	0.3

Table 2. Structural Formula of the Compound

No	Compound Name	Structural Formula	No	Compound Name	Structural Formula
1	Epicatechin	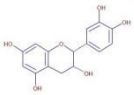	14	Liquiritigenin-7-O-β-D-apiofuranosyl-4'-O-β-D-	
2	Quercetin	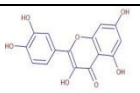	15	glucopyranoside Demethylwedelolactone	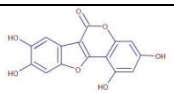
3	Isoquercitrin	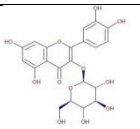	16	(-)-Epicatechin gallate (-)-	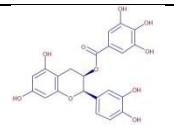
4	Quercetin 3-O-β-D-Glucuronide	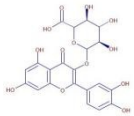	17	Phloretin	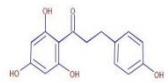
5	Epigallocatechin (-)-	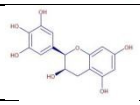	18	Scutellarin	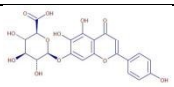
6	Procyanidin B_2	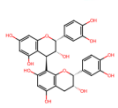	19	Astilbin	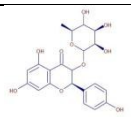
7	Dihydroquercetin	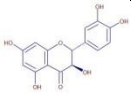	20	Morin	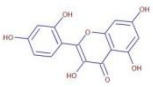
8	Phlorizin	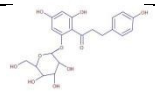	21	Procyanidin B_1	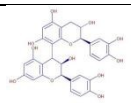
9	Rutin	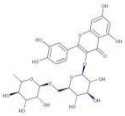	22	2'-O-Galloylhyperin 2'-O-	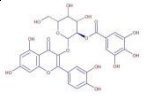
10	Naringenin	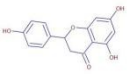	23	Pinocembrin	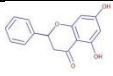
11	Eriodictyol	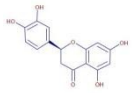	24	(+)-Gallocatechin	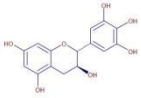
12	Chlorogenic acid	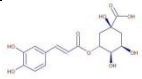	25	Myricetin	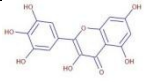
13	Emodin	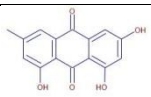	26	Kaempferol-7-O-β-D-glucopyranoside	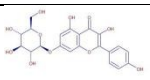

RDP-23's molecular ion peak $[M-H]^{+1}$ is 257.08072, which, based on comparison with the mzVault database, is inferred as Pinocembrin and has the molecular formula $C_{15}H_{12}O_4$. RDP-24's molecular ion peak $[M-H]^{+1}$ is 307.08133, inferred as (+)-Gallocatechin by comparison with the mzVault database, with the molecular formula $C_{15}H_{14}O_7$. RDP-25's molecular ion peak $[M-H]^{+1}$ is 319.04514, which is inferred as

Myricetin by comparison with the mzVault database, corresponding to the molecular formula $C_{15}H_{10}O_8$. RDP-26's molecular ion peak $[M-H]^{+1}$ is 449.10797, inferred as Kaempferol-7-O-β-D-glucopyranoside by comparison with the mzVault database, with the molecular formula $C_{21}H_{20}O_{11}$.

Study on the Antioxidant Activity of *Rosa davurica* Pall (RDP)

Evaluation of DPPH radical scavenging ability

Figure 7(A) illustrates a gradual increase in the scavenging ability of the flavonoid solution towards DPPH radicals as the concentration rises. The purified total flavonoids exhibited notably higher radical scavenging ability than the unpurified form at equivalent concentrations, indicating a positive correlation between antioxidant potency and flavonoid content. The antioxidant efficacy ranked as follows: Vc > purified total flavonoids > total flavonoid extract. Between 0.01 and 0.05 mg/mL, purified substances showed higher DPPH radical scavenging percent than the crude extract at the same concentration, but lower than Vc. At 0.03 mg/mL, the scavenging percent were 91.68% for Vc, 86.97% for purified total flavonoids, and 73.25% for total flavonoid extract. These findings demonstrate that both the RDP extract and isolated compounds exhibited potent DPPH radical-scavenging activity, with a notable increase in flavanol-scavenging efficacy post-purification, primarily due to their flavanol content. The purification procedure eliminates contaminants and enhances the concentration of flavonoids, concentrating on the phenolic hydroxyl groups and other active groups, which can provide hydrogen atoms more effectively to combine with DPPH radicals; at the same time, the higher the concentration, the more flavonoid molecules participate in the reaction, and the more significant the radical scavenging effect.

·OH radical clearance capacity analysis

Figure 7(B) illustrates that the capacity of flavonoid solutions to clear ·OH radicals increased gradually with increasing solution concentration, displaying a concentration-dependent trend. At concentrations ranging from 0.01 mg/mL to 0.05 mg/mL, the clearance percent for Vc, total refined flavonoids, and overall flavonoid extract were 98.68%, 78.4%, and 41.7%, respectively. Both pre-purification and post-purification radical clearance percent for flavonoid solutions were lower than those for Vc, and the purified flavonoid solution consistently exhibited stronger radical clearance than the unpurified ones. Between 0.01 mg/mL and 0.05 mg/mL concentrations, the antioxidant capacity of total refined flavonoids was slightly below that of Vc, indicating a higher antioxidant capacity of the purified flavonoids.

Analysis of O^{2-} free radical clearance capacity

A positive linear correlation was observed in Fig. 7(C) between the concentrations of flavonoid solutions before and after purification and the percent of O^{2-} free radical clearance within the range of 0.1 to 0.5 mg/mL. Upon reaching 0.5 mg/mL, the percent clearances for Vc, total purified flavonoids, and total flavonoid extract were 88.4%, 47.7%, and 44.7%, respectively. Before and after purification, the increase in flavonoid extract concentration led to a corresponding rise in the O^{2-} free radical clearance rate, due to enhanced electron supply capacity for O^{2-} free radicals, resulting from the purification process elevating the active group density. Nonetheless, the efficacy of RDP in O^{2-} free radical clearance was comparatively lower than that against DPPH and ·OH free radicals,

which might be due to glycosylation and improper hydroxyl substitution positions in flavonoid molecules, reducing their clearance of O^{2-} free radicals. The above results indicate that the clearance ability of RDP after purification was significantly enhanced for O^{2-} free radicals. However, the overall clearance ability was weaker than that of other free radicals.

Analysis of $ABTS^+$ free radical clearance capacity

As depicted in Fig. 7(D), the antioxidant activity of the flavonoid solutions against $ABTS^+$ radicals increased gradually with rising solution concentration, both pre- and post-purification. The purified total flavonoids exhibited notably greater $ABTS^+$ radical scavenging capacity compared to the unpurified ones at equivalent concentrations. Notably, at concentrations ranging from 0.004 to 0.008 mg/mL, the purified total flavonoids exhibited superior $ABTS^+$ radical-scavenging activity compared with Vc, suggesting greater antioxidant efficacy at lower concentrations. This is because the purified flavonoid active components have more hydroxyl groups and conjugated structures, with more reaction sites than Vc. A higher percentage of ABTS+ radical clearance can be achieved through the synergistic action of multiple sites and a higher percentage of electron and hydrogen-atom transfer than with Vc. At higher concentrations, the purified total flavonoids exhibited a slightly lower $ABTS^+$ radical clearance capacity than Vc but were nearly equivalent to Vc. At a concentration of 0.02 mg/mL, the clearance percent of Vc was comparable to those of the purified total flavonoids and total flavonoid extract, which were 98.5%, 97.1%, and 87.9%, respectively. The above results indicate that the purification process significantly enhanced the $ABTS^+$ free-radical-scavenging capacity of RDP, especially at low concentrations, with a clearance efficiency that is close to, or even exceeds, that of Vc.

Consistent with previous research findings, this study confirmed that RDP has significant antioxidant potential. Chen *et al*. (2025) demonstrated that RDP exhibited strong antioxidant activity *in vitro*. In recent years, there has been increasing attention paid to the natural sources of antioxidants. Flavonoids are natural compounds synthesized in plants, which can scavenge free radicals and possess strong antioxidant capacity (Luo *et al*. 2025). Li *et al*. (2024) used AB-8 macroporous resin to purify the flavonoids from Longyao Babao. They also confirmed that the purification process could significantly enhance the DPPH radical scavenging ability of flavonoids. Rahman *et al.* (2015) research on the ability of *Tabebuia pallida* leaves to scavenge ·OH radicals. Niu *et al*. (2020) extracted total flavonoids from *Alpinia oxyphylla* using microwave-assisted extraction and conducted an antioxidant activity study. The results showed a good linear relationship between flavonoid concentration and the O^{2-} radical-scavenging rate. Xue *et al*. (2024) purified the flavonoids from *Euphorbia hirta* L. using HPD-300 resin and investigated their antioxidant activity. The results indicated that the purified flavonoids from *Desmodium styracifolium* significantly enhanced the scavenging ability of $ABTS^+$ radicals. Liu *et al*. (2022) verified that three flavonoids isolated from *Patrinia villosa* (Thunb.) Juss exhibited favorable *in vitro* antioxidant activities *via* DPPH and ABTS radical scavenging assays. The above studies have all demonstrated that flavonoids have significant antioxidant activity and are positively correlated with concentration.

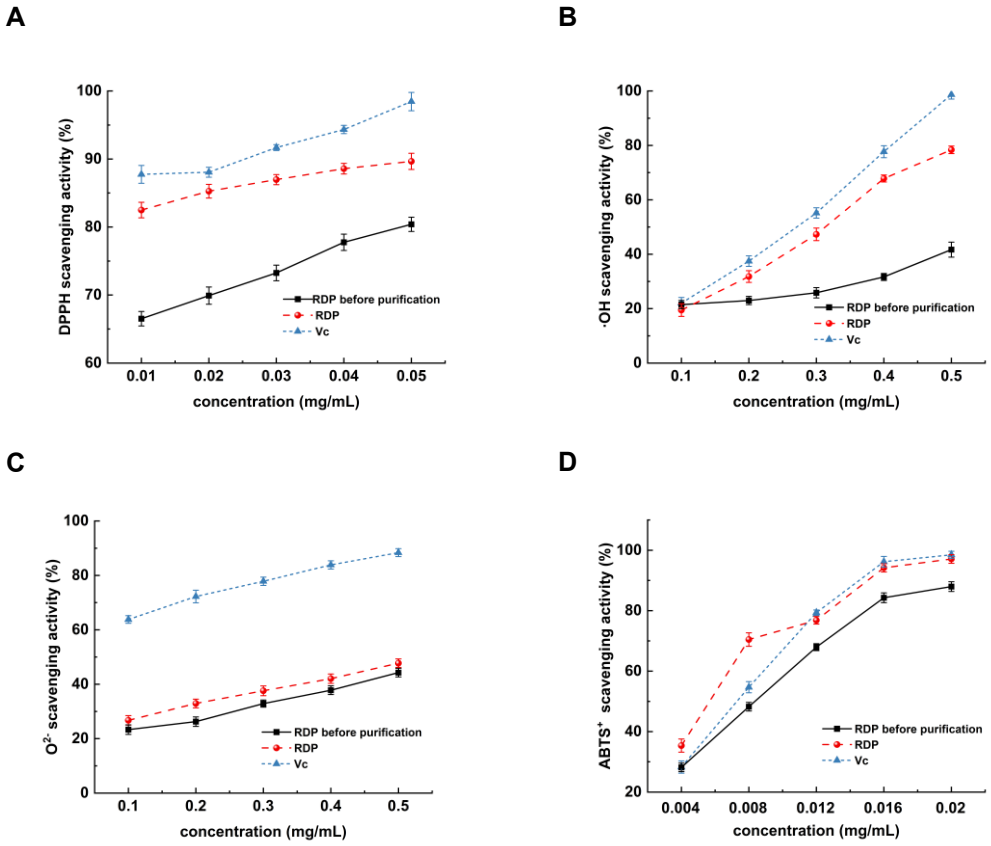

Fig. 6 (A-E). Study on the antioxidant activity of RDP: (A) DPPH radical scavenging ability; (B) ·OH radical scavenging ability; (C) O^{2-} radical scavenging ability; and (D) $ABTS^{+}$ radical scavenging ability

CONCLUSIONS

1. This study optimized the purification process of anthocyanins from *Rosa davurica* Pall using macroporous resin. Through static adsorption and desorption experiments, it was determined that AB-8 resin was the best purification carrier. The optimal process was a sample loading flow rate of 2.0 mL/min, a sample loading concentration of 0.5 mg/mL, pH 5, and a sample loading volume of 90 mL. The elution was performed with 70% ethanol at a flow rate of 2 mL/min for 100 mL. The purity of the anthocyanins increased from 19.25% to 62.86 ± 0.82%, representing a 3.2-fold increase. A total of 26 anthocyanin components were identified using HPLC-MS. *In vitro* antioxidant experiments demonstrated that the anthocyanins from *Rosa davurica* Pall exhibited excellent scavenging activity against various free radicals and high total reducing power, and this effect was concentration-dependent, confirming its potential application in antioxidant research.
2. This article has reported on the qualitative analysis of *Rosa davurica* Pall (RDP). However, quantitative analysis of the 26 flavonoid components has not yet been carried out. In the future, HPLC-MS/MS can be used to establish a multi-component

quantitative method. Using network pharmacology and molecular docking, the synergistic effects among components can be analyzed, and the antioxidant mechanisms in cells and animal models can be further explored. The results showed that purification only slightly improved the antioxidant activity of RDP. Thus, the purification step can be omitted or simplified in practical production to save time and cost, without obvious loss of antioxidant performance.

ACKNOWLEDGMENTS

The authors express their sincere gratitude to the Engineering Research Center of Forestry Biotechnology in Jilin Province, China, for its valuable assistance with the structural analysis of flavonoids from *Rosa davurica* Pall.

Conflict of Interest

The authors declare that they have no conflicts of interest.

Use of Generative AI

No generative artificial intelligence (AI) tools were used in the preparation of this manuscript.

Funding

This work was supported by the fund of the Jilin Provincial Department of Science and Technology to Yanqiu Liu (No.20230101246JC).

REFERENCES CITED

Cao, J., Peng, L. Q., Du, L. J., Zhang, Q. D., and Xu, J. J. (2017). "Ultrasound-assisted ionic liquid-based micellar extraction combined with microcrystalline cellulose as sorbent in dispersive microextraction for the determination of phenolic compounds in propolis," *Analytica Chimica Acta* 963, 24-32. https://doi.org/10.1016/j.aca.2017.01.063

Chen, L., Abudureheman, B., Anwar, O., Abdugini, E., Zhang, J., Tang, R., Gao, Z., Pan, H., and Ye, X. (2025). "Extraction, purification, component analysis and bioactivity of polyphenols from *Artemisia dracunculus* L.," *Foods* 14(10), article 1823. https://doi.org/10.3390/foods14101823

Diao, Y., Yu, X., Zhang, C., and Jing, Y. (2020). "Quercetin-grafted chitosan prepared by free radical grafting: Characterization and evaluation of antioxidant and antibacterial properties," *Journal of Food Science and Technology* 57(6), 2259-2268. https://doi.org/10.1007/s13197-020-04263-2

Gao, C., Du, K., Wen, J., Li, H., Liu, W., Zheng, Y., Han, M., Li, X., and Chang, Y. (2025a). "Green extraction of bioactive flavonoids in *Scutellariae radix* using deep eutectic solvents-based ultrasound-assisted matrix solid phase dispersion combined with computer-aided analysis," *Journal of Chromatography A*, 1751, article 465938. https://doi.org/10.1016/j.chroma.2025.465938

Gao, H. Y., Liang, M., Xiao, R. P., Wei, H., Li, W. Y., Yang, H., Song, M. J., Lei, X. J., and Zhang, N. Q. (2025b). "Chemical composition, antioxidant activity of

Acanthopanax sessiliflorus leaves extract," *Chemistry & Biodiversity* 22(9), article e202500231. https://doi.org/10.1002/cbdv.202500231

Hwang, D. H., Asirvatham, R. D., Mohan Prakash, R. L., Kang, C., and Kim, E. (2024). "Therapeutic potential of *Rosa davurica* Pall. root extract as an antidiabetic agent: A comprehensive analysis from molecular mechanisms to *in vivo* efficacy," *International Journal of Molecular Sciences* 25(16), 8944. https://doi.org/10.3390/ijms25168944

Kim, H. M., Park, Y. A., Lee, E. J., and Shin, T. Y. (1999). "Inhibition of immediate-type allergic reaction by Rosa davurica Pall. in a murine model," *Journal of Ethnopharmacology* 67(1), 53-60. https://doi.org/10.1016/s0378-8741(99)00013-6

Li, N., Wu, X., Yin, Q., Dong, Z., Zheng, L., Qian, Y., Sun, Y., Chen, Z., and Zhai, K. (2024). "Extraction, identification, and antioxidant activity of flavonoids from *Hylotelephium spectabile* (Boreau) H. Ohba," *Foods* 13(17), article 2652. https://doi.org/10.3390/foods13172652

Liu, Y. C., Sui, N., Wang, J. Q., Wang, X., Liu, W., Xiang, Z., and Chen, C. L. (2022). "A novel flavonoid with antioxidant activity from *Patrinia villosa* (Thunb.) Juss," *Natural Product Research* 36(12), 2977-2983. https://doi.org/10.1080/14786419.2021.1935931

Liu, C., Yu, X., Zhang, M., Wang, S., Ni, J., Yuan, X., and Han, H. (2024). "Antioxidant and hepatoprotective effect of *Rosa davurica* Pall seed oil on CCl4-induced acute liver injury in mice," *Journal of Medicinal Food* 27(7), 636-650. https://doi.org/10.1089/jmf.2024.K.0018

Luo, J., Pang, Y., Liu, D., Sun, J., and Bai, W. (2025). "Optimization of flavonoid extraction from *Tarocco* orange (*Citrus sinensis* [L.] Osbeck) peel using supercritical CO_2 followed by ethanol: chemical composition, antioxidant, and antibacterial activities," *Journal of the Science of Food and Agriculture* 105(15), 8958-8971. https://doi.org/10.1002/jsfa.70136

Nguyen, T. L. A., and Bhattacharya, D. (2022). "Antimicrobial activity of quercetin: An approach to its mechanistic principle," in: *Molecules* 27(8), 2494. https://doi.org/10.3390/molecules27082494

Niu, Q., Gao, Y., and Liu, P. (2020). "Optimization of microwave-assisted extraction, antioxidant capacity, and characterization of total flavonoids from the leaves of *Alpinia oxyphylla* Miq," *Preparative Biochemistry and Biotechnology* 50(1), 82-90. https://doi.org/10.1080/10826068.2019.1663535

Rahman, M. M., Islam, M. B., Biswas, M., and Khurshid Alam, A. H. (2015). "*In vitro* antioxidant and free radical scavenging activity of different parts of *Tabebuia pallida* growing in Bangladesh," *BMC Research Notes* 8, article 621. https://doi.org/10.1186/s13104-015-1618-6

Shen, C. Y., Hao, Y. F., Hao, Z. X., Liu, Q., Zhang, L., Jiang, C. P., and Jiang, J. G. (2021). "Flavonoids from *Rosa davurica* Pall. fruits prevent high-fat diet-induced obesity and liver injury *via* modulation of the gut microbiota in mice," *Food & Function* 12(20), 10097-10106. https://doi.org/10.1039/d1fo01373d

Thupakula, S., Nimmala, S. S. R., Dawood, S. M., and Padiya, R. (2024). "Synergistic anti-diabetic effect of phloroglucinol and total procyanidin dimer isolated from *Vitis*

vinifera methanolic seed extract potentiates *via* suppressing oxidative stress: *In-vitro* evaluation studies," *3 Biotech* 14(3), 76. https://doi.org/10.1007/s13205-024-03929-4.

Xue, X., Guo, L., Ai, L., Li, L., Liu, W., Li, P., and Sheng, Z. (2024). "Enrichment and purification of flavonoids from *Euphorbia hirta* L. and antioxidant activity evaluation," *Pakistan Journal of Pharmaceutical Sciences* 37(4), 881-890. https://doi.org/10.36721/PJPS.2024.37.4.REG.881-890.1

Yi, Z. Y., Zhang, M., Wang, S., Liu, S. Y., Bai, L. C., Liu, C. Y., Han, H., Shu, Z. P., and Yu, X. J. (2025). "Discovering the active components of *Rosa davurica* Pall on ameliorating acute myocardial ischemia based on spectral relationships, network pharmacology, molecular docking and molecular dynamic," *Fitoterapia* 184, 106648. https://doi.org/10.1016/j.fitote.2025.106648

Zhang, Y., Hao, X., Zhao, L., Xiang, L., and Wang, C. (2025). "Synthetic biology of terpenoid and flavonoid natural food additives: Research progress and future challenges," *Journal of Agricultural and Food Chemistry* 73(44), 27836-27854. https://doi.org/10.1021/acs.jafc.5c05422

Zhang, H., Li, X., Wu, K., Wang, M., Liu, P., Wang, X., and Deng, R. (2016). "Antioxidant activities and chemical constituents of flavonoids from the flower of *Paeonia ostii*," *Molecules* 22(1), 5. https://doi.org/10.3390/molecules22010005

Zhao, C., Xu, J., Liu, Y., Xu, P., Yi, J., Feng, L., Miao, Y., and Zhang, Y. (2024). "Extraction and purification of flavonoids and antiviral and antioxidant activities of *Polygonum perfoliatum* L.," *Molecules* 30(1), 29. https://doi.org/10.3390/molecules30010029

Article submitted: February 2, 2026; Peer review completed: April 22, 2026; Revised version received and accepted: June 2, 2026; Published: June 25, 2026.
DOI: 10.15376/biores.21.3.7454-7474